ORIGINAL PAPER

The susceptibility analysis of landslide using bivariate and multivariate modeling techniques in western Algeria: case of Fergoug watershed (Beni-Chougrane Mountains)

Zaagane Mansour[1,2] • Thiery Yanick[3,4] • Safa Aissa[5,6] • Refas Soraya[1,2] • Hamimed Abderahmane[1] •
Abbache Abdelkader[1,7] • Khaldi Abdelkader[1,2] • Souidi Zahéra[1] • Mouassa Souad[1,2] • Moussa Kacem[5,8]

Abstract

Landslides are considered to be the most important and frequent natural events causing considerable damage. Many areas in Algeria and elsewhere in the world are affected by this type of phenomenon. Located in the Tellian Chain of the Northwest of Algeria, Fergoug watershed is largely affected by several landslide events that led to (siltation of dams and roads, bridges, and buildings destruction). The damage cost amounted to hundreds of thousands of dollars and sometimes exceeds the reaction of the authorities concerned. In order to help local authorities in their prevention approach, a landslide sensitivity map has been realized using different models: (i) the frequency ratio (FR), (ii) the linear multiple regressions (MLR), and (iii) the information value model (IVM). The landslide inventory was established and includes 142 landslides and 10 conditioning factors (slope angle, slope aspect, profile curvature, distance to rivers, roads, faults, earthquakes, land use, lithology, and precipitation). These factors were prepared from several multisource data sources. The results were validated using the operating characteristic of the receiver and the areas under the curves obtained using the methods FR, IVM, and MLR are respectively 0.87, 0.83, and 0.81. It is proposed that the landslide susceptibility map produced from the FR model be more useful for the study area. The results demonstrate that for the frequency ratio model, the very high, high, moderate, low, and very low susceptibility classes are 58%, 24%, 5%, 2%, and 9.5%, respectively. Almost 73 landslides events are situated along the Fergoug River. These results could reveal the relative importance of different factors in explaining landslides and help engineers plan land use planning.

Keywords Landslide · Susceptibility map · Fergoug watershed · Conditioning factors · Risks · Western Algeria

✉ Zaagane Mansour
zaagane@yahoo.fr

1 Mascara University, Bpox 305 Road of Mamounia,
29000 Mascara, Algeria

2 Laboratory of Research on Biological Systems and Geomatics
(LRSBG), Bpox 305 Road of Mamounia, 29000 Mascara, Algeria

3 BRGM, 3 Avenue Claude Guillemin, 45100 Orléans, France

4 Risks and Prevention Department (RPD), BRGM,
45100 Orléans, France

5 Mohamed Ben Ahmed University, Oran II, 31000 Oran, Algeria

6 Laboratory of Hydrogeology (LH), Mohamed Ben Ahmed,
University, Oran-2, Oran, Algeria

7 Laboratory of Paleontology, Stratigraphy and Paleo-Environments,
Mohamed Ben Ahmed University (Oran II), Oran, Algeria

8 Laboratory of Basins Geodynamic and Sedimentary Balance Sheet
(GeoBaBiSe), Oran II University, 31000 Oran, Algeria

Introduction

Slope movements are considered to be one of the main hazards and risks in mountainous areas (Van Westen et al. 2006). Among these phenomena, landslides and rock-fall are the most widespread. They are characterized by the displacement of a more or less coherent materials (soil, marls, clays ora mixture of several type of materials) or rocks (blocks, rocks) along a shear surface induced by gravity effect (Dikau 1999; Palucis et al. 2018; Chattoraj et al. 2019). These phenomena can be called as slope failures because the underlying debris that holds the slope in place fails to maintain stability due to the large thrust exerted by the mobilized land (Solaimani et al. 2013). Their velocity and intensity may depend on the nature of the displaced materials as well as the slope gradient (Mahdadi et al. 2018; Cui et al. 2019). Slow moving landslides (i.e., with a velocity of few centimeters per year) can

seriously damage infrastructures, especially when volumes are significant (Frattini et al. 2018). Rapid landslides provide little warning and cause a large impact, especially near developed areas (Marc et al. 2015; Zygouri and Koukouvelas 2019). Landslides are considered a major risk in the world and they can be disastrous for human life and property (Van Westen et al. 2011). According to the rate mortality, these phenomena represent approximately 9 % of all natural risks in the world (Mousavi et al. 2011) and cause approximately 1000 deaths per year worldwide and approximately four billion (dollars) property damage only in the USA (Lee and Pradhan 2007).

Algeria is one of the countries that are widely affected by these phenomena. Landslides have seriously affected housing and various infrastructures (buildings, roads, bridges, dams, and railways) during the last twenty years (Mahdadi et al. 2018; Karim et al. 2019). Coastal and mountainous zones are the most landslide prone areas of the country (Lee and Pradhan 2007). Each year, especially in winter, extreme rainfalls cause significant landslides affecting the roads in mountainous regions and cause the isolation of several hundred homes. In recent years, remedial works have been carried out to repair damages on the roads with hundreds of thousands dollars spent by the government (Manchar et al. 2018). Because the potential problems induced by landslides are related to poor slope planning and little attention by end-users, the Algerian authorities are warned against the damages induced by landslides and the seriousness of their management and prevention. Therefore, recently, the authorities have highlighted the need to consider this hazard in local development planning. Some efforts have been made to identify phenomena location, improve the inventory with the characteristic of phenomenon, and prevent their occurrences the main goal is to produce landslide susceptibility, hazard, and risk maps for specific areas.

Located in the northern fringe of Algeria, the Fergoug watershed is very prone to landslides affecting infrastructures. In order to follow the government instructions and to improve the landslide mapping practices for regular objectives, we are interested in how to map landslide susceptibility with simple data-driven methods based on available data. The defined methodology should be easily reproducible and easily understandable by local authorities to be applied on other territories. To carry out this work, the Fergoug watershed was chosen as a case study to assess the susceptibility using three methods answering the above-mentioned points namely: the frequency ratio method (RF), the value of information method (IVM), and multiple linear regression method (MLR). After a sensitivity analysis of the different spatial variables on the models, the best maps obtained for each approach are compared through two statistical tests. The results are discussed in order to choose the most adapted

approach to the local context. The best map obtained could be used as a basic support for planning small or large projects while avoiding areas highly exposed to landslides.

Study area

The Fergoug watershed, covering an area of 169 km^2, is located in the Beni Chougrane Mountains, which is part of the western Tellian Chain of Algeria (Fig. 1a). This young mountain area was structured during the Alpine phase and slowly continues to structure itself (Upper Miocene) (Thomas 1985). These mountains rise from 50 m (a.s.l.) near Mohamadia from 935 m (a.s.l) near Chareb Errih in the east of Mascara. Structurally, the two plains (Ghriss and Habra) are separated by the very tectonized ridge of the Beni-Chougrane mountainous in which the Fergoug watershed is part (Fig. 1a).

The Fergoug watershed is located northeast of the Tessala Mountains, south of Mohamaddia on the axis of the Macta River (Fig. 1a). The morphology of the study area is irregular with mountainous areas on either side of the Macta River (Fig. 1b). These mountains are cut by a network of fairly dense rivers sometimes feeding directly into the Fergoug dam, making this dam the collection point for rainwater discharged by tributaries of the main wadi (Fergoug, (Thaghzout and Hammam; Fig. 1c, d). Among this dense network, it is possible to observe small plains corresponding to ancient fluvial terraces (Fig. 1b). These mountains have a typical Tellian direction with an ENE / WSW orientation coinciding with the anticlinal fold systems affecting northern Algeria. This area is also affected by faults of various nature and direction ranging from N140° (along which the main wadi of Fergoug is located), N70° to N20°. They are represented respectively by dextral or senestral strike slip and reverse faults sometimes limiting the folded structures. The anticlines reveal an ancient core represented by friable Cretaceous formations, notably marl and marl-limestone (Fig. 2b). In the center, the lithology consists of friable Miocene rocks such as marls, sandy clays, clays, and sandstone clays. These formations are overlain by hard Pliocene rocks (sand, sandstone, and limestone) forming the main ridges (Fig. 2a). The soils derived from the weathering of these soft Miocene materials are rich in swelling clays favorable to runoff when surface conditions permit (Stark and Hovius 2001; Zaagane et al. 2015), particularly when the Mediterranean-influenced climate manifests itself in the form of violent thunderstorms with intensities greater than 100 mm h^{-1}. These particular episodes can be frequent especially in autumn and winter when vegetation cover is very limited (Mekerta et al. 2008).

A characteristic feature of the manifestation of these intense rainfalls on an arid Mediterranean landscape is the
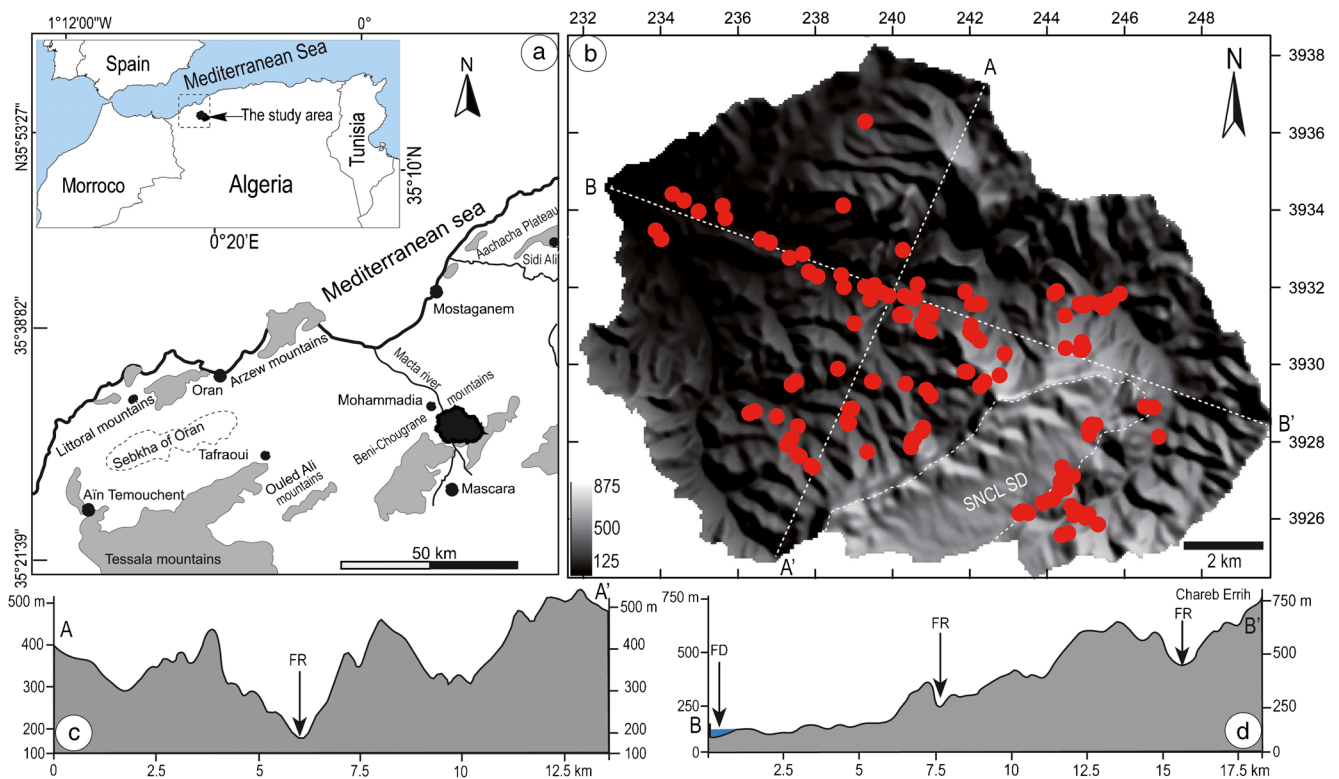
Fig. 1 Geographic and geomorphologic frameworks of the study area, a: map showing the western Tellian chain related to the Northern part of Algeria (small map in the left corner), b: Digital elevation model showing the topographic features of the study area, the red circles represent the landslides locations, the white dashed line represents the Sidi Daho Synclinorium (SNCL SD); c and d: topographic cross section related to the dashed line in b. The abbreviations FR and FD are respectively Fergoug River and Fergoug Dam

development of badlands. These erosion processes have been widely described in the literature and generally attributed to environmental changes (Cánovas et al., 2017; Mosavi et al. 2018). These changes are induced either by climatic oscillations or by prioritized human activity, which leads to increased runoff due to vegetation cover degradation (Roose et al. 1993). These environmental conditions of a degraded Mediterranean environment are also conducive to the initiation of landslides affecting many infrastructures in two ways:

(i) Directly: for example on the road connecting Mascara to Mohamadia, many cases of destruction were observed (Fig. 3). Landslides affect the roadways, generally located on slopes more or less steep, mobilizing few part or large part of the road (Fig. 3a, b, c, d).

(ii) Indirectly: the landslides join the erosion areas along the banks of the Fergoug River mobilizing a large part of the land. Materials are transported during floods towards the Fergoug dam located downstream, thus causing its silting (Fig. 4). These landslides are triggered in different environments along the main course of the Fergoug River on dense forest cover (Fig. 4a, b) or in upstream

tributaries, affecting both bare ground (Fig. 4c) and ground with temporary vegetation cover (Fig. 4d, e).

Landslide susceptibility mapping: background and description

The production of a landslide susceptibility maps is the first step in the landslides risk assessment (Corominas et al. 2014). Over the past decade, advances in modeling and geographic information systems (GIS) have provided several of quantitative methods for mapping susceptibility to landslides (Van Westen et al. 2006). Various quantitative models have been successfully implemented with several datasets representing the predisposing factors (Reichenbach et al., 2018). These models are based on the assumption that landslides follow common environmental, physio-geographical, and geotechnical behaviors under similar conditions in the past, present, and future (Ghimire 2011; Corominas et al. 2014). To achieve correctly a landslide susceptibility map by a quantitative method, a preliminary stage requires the preparation of a
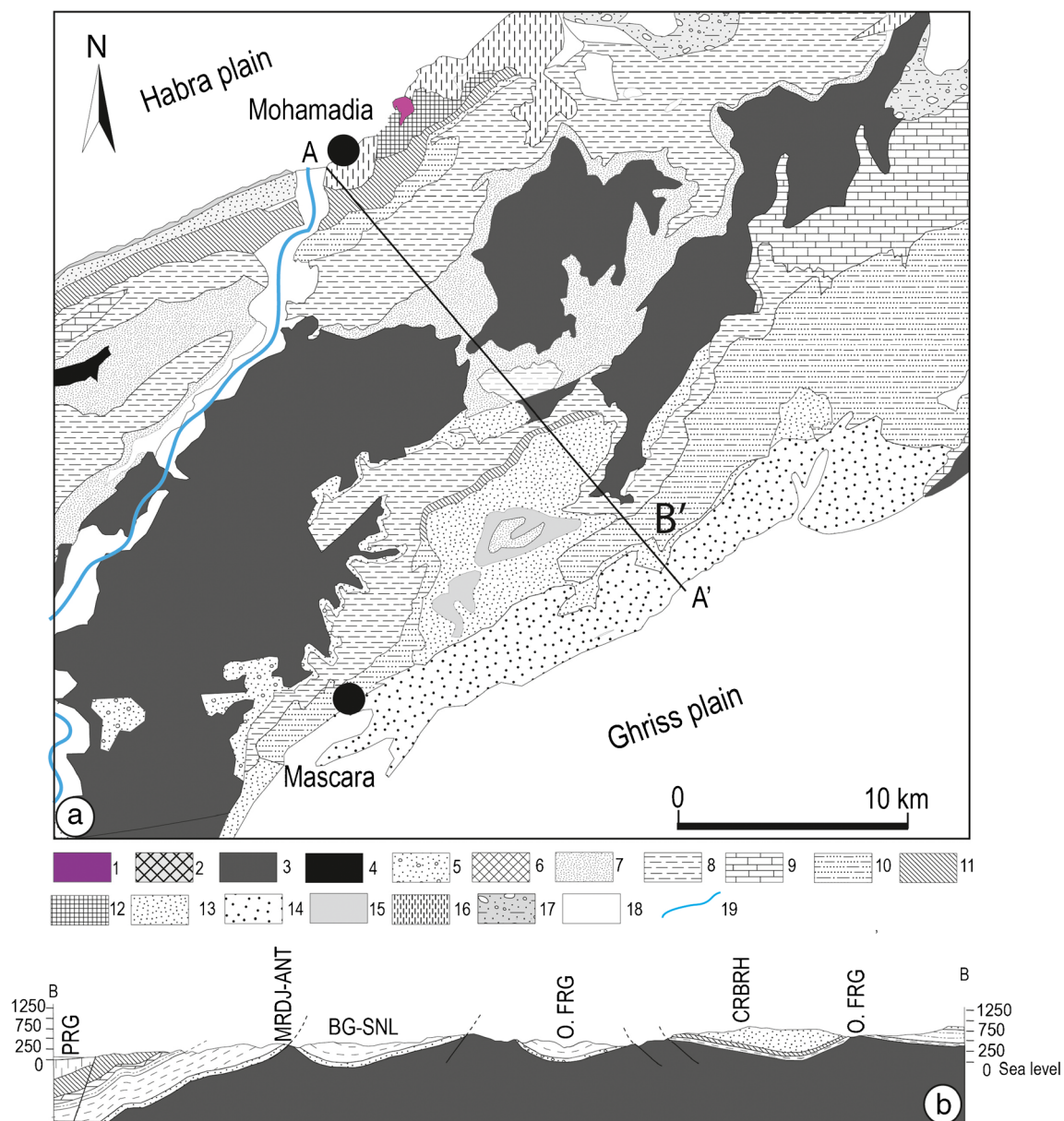
Fig. 2 Geological map of the Beni-Chougrane Mountains (geographic coordinates) a: 1, eruptive rocks; 2, Jurassic limestones; 3, ante-nappes formations; 4, marl (early Miocene); 5, conglomerate and sandstone (early Miocene); 6, continental formation of Bou Hanifia; 7, basis sandstone; 8, Bleu marl; 9, Lithothamniees limestone; 10, El Bordj sandstone formation; 11, diatomitic formation; 12, gypsyfour and marly gypsifourous; 13, bleu marl; 14, sea sandstone; 15, continental sandstone and silt at Helix; and 16, lake deposit; 17, limestone crust; 18, alluvium; 19, watercourse. The black line disposed perpendicular to the alignment of the chain represents the geological cross section, b: geological cross-section along the Beni-Chougrane Mountains showing the geologic features (before and after-nappes). For the abbreviations, ANT is and SNL are respectively anticline and synclinal, BG is Bel Ghrib, MRDJ is Merdja, CRBH is Cherb Errih. FRG is Fergoug; PRG is Mohamadia O. is Oued e.g (Wadi or rivers)

database about the landslides, with an inventory compiling several information (i.e., location, typology, activity, and morphometric indexes) (Zaagane et al. 2015; Thiery et al. 2020) and different maps representing the predisposing factors. Once the data prepared, the inventory is confronted with the different factors listed (Fig. 5) in order to establish the relationships between events and the most influential factors

Depending on the approach chosen, the results may differ (Thiery et al., 2007). It is sometimes necessary to compare certain approaches with other in order to choose the best one suiting the study site and the different field observations (Thiery et al. 2014). In this study, the choice of the reliable susceptibility map suitable for the study area was guided by the degree of performance of the model used in the

Fig. 3 Roads affected by landslides in different location, a: road connecting Mascara to Mohamadia affected as a whole by a large landslide (dark line represents the road which leads from Mascara to Mohamadia), b: the landslide seen from one top, the dashed lines show the limits of the landslide area, c: the cliff corresponds to the rupture zone, even the device designed to protect the road was affected by the great thrust generated by landslide, c: landslide affecting part of the road connecting Ain Fares Mohamadia in which we can see the beginning of a slip affecting thisroad recently built, dashed lines are related to cracking relatives to the rupture zone. The black and white arrows show the direction of movement of the materials

development of the final map. To compare them, the best way is to use the same dataset and the same strategy of calibration, validation with simple tests of comparison. In Figure 5, we illustrate the strategy used for this study. Results can be used as a basic support showing the probability of occurrence of landslides according to different susceptibility classes (Guzzetti et al. 2012; Caiyan and Jianping 2009; Pradhan and Lee 2010; Erzin and Cetin 2013; Pourghasemi et al. 2012; Karim et al. 2019) (Fig. 5). Among these methods, bivariate and multivariate methods (Pourghasemi et al. 2012; Lari et al. 2014; Hungr 2018; Robbins 2016; Nsengiyumva et al. 2019) become standards in the scientific community for mapping landslide susceptibility at regional and local scales (Thiery et al. 2020). Bivariate methods have the advantages to explore simply the relationships between landslides and factors or combination of factors. They are simple to implement and yielding results easily understood by practitioners. Multivariate methods can be a little bit more complex to implement because they need, sometimes, the used of specific statistical packages, and need to explore positive relationship of landslides and non-landslides. Moreover, they are more difficult to explain to end-users. Nevertheless, for both methods, their degree of prediction based on the analysis of phenomena taken and not taken into account in the calibration phase is generally higher than 80%, especially if the data used are accurate and validated by the expert.

Therefore, three data-driven methods have been selected with two bivariate (the frequency ratio — FR, and the information value — IVM) and one multivariate method (the multiple linear regression method — MLR). The goal is to choose the best suitable method for the test site.

Frequency ratio model

The frequency ratio model (FR) has been applied for several case studies in order to predict areas likely to generate landslides (Yalcin et al. 2011; Park et al. 2013; Pradhan and Lee 2010; Manchar et al. 2018; Gholami et al. 2019). The frequency ratio, as a leading probability model, is based on the observed spatial relationships between spatial distribution of landslide and causal factors. It is used especially to reveal the correlation between landslide locations and the factors in
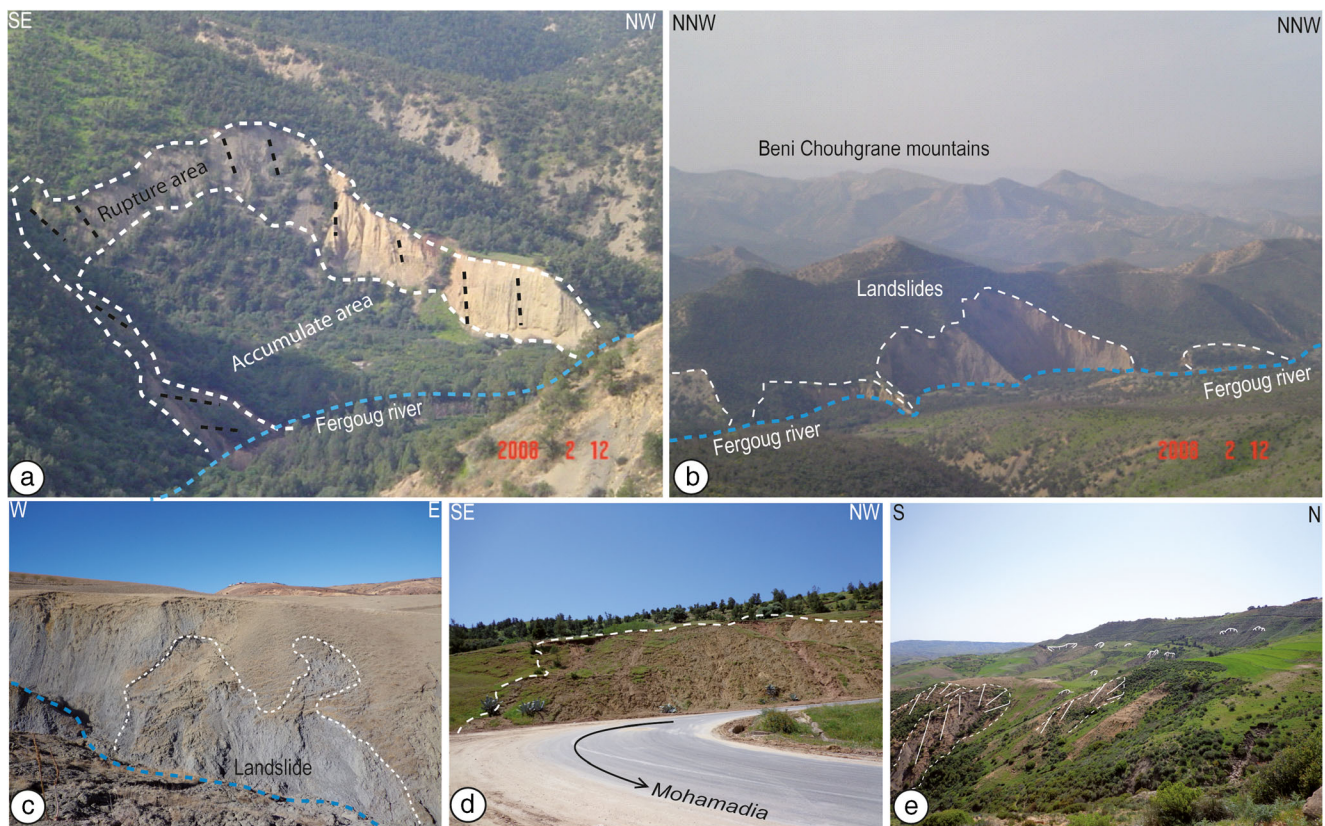
Fig. 4 Several landslides happened along the Fergoug river, the moved material is transported by fluvial waters to the Fergoug Dam during the floods season, a: important landslide characterized by the presence of a dense forest cover and b: landslide happened along river not far from the Fergoug dam, c:Miocene marl affected by a small landslide not directly in the Fergoug River it happened on one of its tributaries, d: soils moved because a landslide close to the road and e: many landslide located in the oriental slope in the central part of the study area

the study area. Consequently, the FR can be used to quantitatively assess the landslide susceptibility.

Technically speaking, FR is based on the association between landslides and predisposing factors with the computation of a ratio between the number of landslides in a predisposing factor class, the total number of landslides, the area of a predisposing factor class, and the total area of the predisposing factor (Lee and Pradhan 2007). Then, FR can be
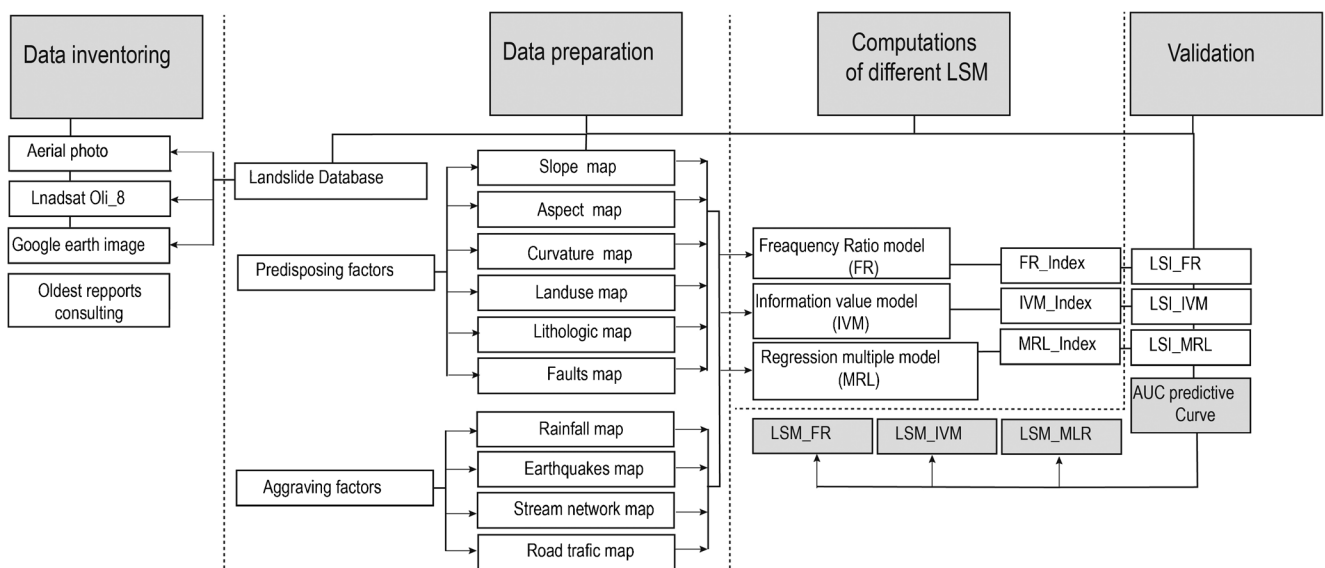

Fig. 5 Overall methodology flowchart showing different stages of process such as data inventorying, data preparation, computations of differents LSM and validation

compute using Eq. (1):

$$FR = \frac{N\frac{p}{i}/N}{N\frac{lp}{i}/N^l} \qquad (1)$$

Where $N\frac{p}{i}$ is the number of cells with landslides in factor class i, N is the total number of cells with landslides. $N\frac{lp}{i}$ is the total number of cells (i.e., with and without landslides) of factor class i, N^l is the total number of cells (i.e., with and without landslides) in the entire study area (Javier and Kumar 2019).

Once the ratio of each independent factor class was calculated, the landslide susceptibility index (LSI_FR) is obtained by summing all (FR) of all factors, as indicated in Eq. (2) (Yilmaz 2010):

$$LSI\_FR = \sum FRj \qquad (2)$$

Where $j = 1$ to n, and n is the total number of factors.

The model obtained shows the degree of correlation between landslides and independent factor class. The higher value of the ratio (FR > 1) shows the large relationship between the landslides occurrence and the factor class; however, a lower ratio value (FR < 1) indicates a low probability of landslide occurrence (Yalcin et al. 2011).

The information value model

The information value model has been widely used to map sensitivity to landslides. For instance, in 2012, Pereira and his colleagues used the Information Value Model (IVM) to assess the role of different combinations of causative factors in the triggering of shallow landslides in different parts of northern Portugal. Many authors have found that the value of information (IVM) model is very useful to define the degree of influence of the individual causative factor responsible of landslides (Champatiray 2000; Arora et al. 2004; Champatiray et al. 2007; Kanungo et al. 2009; Caiyan and Jianping 2009; Pereira et al. 2012; Balsubramani and Kumaraswamy 2013; Passang and Kubíček 2018).

The principle is very close the FR method. It is based on the determination of the influence of each class of predisposing factors on the onset of landslide in a given area. In this model, the information has the value IVM for a class in a thematic layer as indicated in the following equation (Chen et al. 2019):

$$IVM = \log\left(\frac{\text{Conditional probability}}{\text{Prior probability}}\right)\left(\frac{\frac{Si}{Ai}}{\frac{S}{A}}\right) \qquad (3)$$

Where Si is a number of landslide pixels in factor class i, Ai is the number of pixels in a given class i, S is a total number of landslide pixels in the study area, and A is a total number of pixels in the entire study area. The weights of all factor classes were calculated through the ratio of landslide density of each factor class to the landslide density of total area, or the information value can provide the landslide probability in each class and in the total area (Table 1). If IV > 0.1, the factor classes will have the highest probability of landslide occurrence, but factor classes with negative values indicate the presence of a factor with no significant contribution to landslide occurrence. The landslide susceptibility index (LSI) was calculated as follows:

$$LSI\_IVM = \sum_{i=1}^{M} X_{ij} * IVM \qquad (4)$$

Where $X_{ij} = 1$ is the class i exist in factor j and 0 if class i does not exist in factor j, M is the number of class considered (Passang and Kubicek 2018).

Multiple linear regressions

MLR method is one of the first multivariate method applied to assess and to map landslide susceptibility. The method was used in different regions of the world (Felicísimo et al. 2013; Onagh et al. 2012; Felicísimo et al. 2013; Erzin and Cetin 2013). The multiple regression model for some authors appears as an alternative to the bivariate method with better results. This method shows that the sensitivity of landslides changes with the standard deviation of independent and predictor variables (Yalcin et al. 2011). However, some studies show very similar results.

In statistics, MLR is a mathematical regression method that extends simple linear regression to describe changes in a dependent variable associated with changes in several independent variables following this equation (Lee and Sambath 2006):

$$LSI\_MLR = a_0 + a_1X_1 + a_2X_2 + \ldots + a_nX_n + \varepsilon_i \qquad (5)$$

Where εi is the error of the model which expresses or summarizes the missing information in the linear explanation of the values of LS*I*_MLR from X_1, ..., X_n (specification problem, variables not taken into account, etc.). The coefficients a_0, a_1, ..., a_n are the parameters to be estimated.

Data and modeling strategy

The strategy used to assess landslide susceptibility and to obtain the best landslide susceptibility map is split in 4 steps

Table 1 Summary of different types, levels, and complexity of landslide susceptibility and hazard zoning according to the objectives (modified from Fell et al., 2008), where TU = available for any use, MSP = available for public utility mission; P = paying service; SD = on request; CNTS = National Space Technical Center, SPC = Bridge and roadway service, SF= Forestry service; SCGA = Geologicl servey of Algeria; +++ =essential; ++ = important; (*) = precaution (data verification); (**) = verification of the scale of application; I = inventory; S = susceptibility; A = hazard

Thema	Data to use		Disponibility	Organization responsible for data	Domain of use	Hazard application	
	Type	Product				Importance	Precautions
Landslide Inventory	Topographic maps	Scan 1/25000	P	CNTS	I	++	*
	Aerieal Photos	Ortho 1/20000	P	CNTS		+++	**
	Satelites images	30 m/pixel (Oli_8)	TU	MSP		+++	**
	Oldest reports	Bridge and roadway (2018)	SD	SPC		++	**
	Google earth	Images (2019)	TU	MSP		+++	**
	Field verification	/	/	/		+++	**
Topographic data and derived maps	Altemetric data/DEM(SRTM)	30 m/pixel	TU	MSP	I/A/S	+++	*
Geology	Geologic map	Scanned map (1/50000)	SD	SCGA	A/S	+++	*
	Faults lineaments maps	Photo interpretation of satelite images	TU	MSP		+++	**
	Seismic source map	Data base ANSS/NEIC	TU	MSP		+++	**
Hydrology	Stream network map	Extraction for DEM (30m/pixel)	TU	MSP		+++	**
Land use	Forestry map	Scanned map	SD	SF	A/S	++	*
	Photo interpretation of satelite image	Supervised classification (Red/Infra-red images)	TU	MSP		+++	**
Anthropic factor	Roads	Extracted from google earth image	TU	MSP		+++	**
Meteorologic data	Precipitation data	Rainfall data	SD	Weather/Algeria	A/S	+++	**

with: (i) the development of a new inventory of phenomena; (ii) the preparation of spatial variables represented by predisposing factors and aggravating factors; (iii) computations of different landslide susceptibility maps with the three selected methods; (iv) validation of results and comparison of maps.

Landslide inventory

Landslide inventory is a key step to assess landslide susceptibility and hazard (Lee and Pradhan 2013). Several authors as Gzzetti et al. (2006), Corominas et al. (2014) and Thiery et al. (2020) consider this operation as a basic element for all work aimed at the susceptibility mapping. In the Fergoug watershed, the landslide inventory is based on diachronic interpretations (Nichol and Wong 2005; Guzzetti et al. 2012) of aerial and satellite imageries (Landsat imagery and under Google Earth) taking into account of the resolution and the characteristics of each imageries (i.e., tonal, contrast, size, shape, and shadow, as well as contextual indicators such as position and direction of phenomena; Liu et al. 2004). The remote sensing inventory has been completed by field investigations and deep consultation of old reports.

One hundred forty-two landslides have been identified, recorded, and mapped. Several information relating to landslides have been recorded in a spatial database, with (i) the geographic situation, (ii) the typology (translational, rotational, solifluxion and muddy flow), (iii) the surface (in km^2), and (iv) all the factors involved in its initiation. The majority of landslides identified not exceeded an area of $0.01\ km^2$ (89% of landslides < 1 ha) while $10.56\% > 0.01\ km^2$ with an area reaching up to $0.0749\ km^2$. The total area of the landslides identified is approximately $11.14\ km^2$, which represents approximately 6.61% of the entire surface of study area. Phenomena affecting this area can be superficial < 20 m or deep > 20 m. According to their form, (i) 119 cases landslides are translational located upstream of the Fergoug River or (ii) 23 cases are rotational located mainly along the same river (Fig. 1b).

Conditioning factors

The causes of the triggering and occurrence of landslides are truly complex and diverse. There is not a clear agreement to the precise reasons for their manifestation (Corominas et al. 2014). The complex nature of landslide development has led many researchers to study how the occurrence of landslides could be affected by various conditioning factors (Mugagga et al. 2012). Among them, we quote predisposing factors with

(i) topographic factors (e.g., slope, aspect, curvature) and geological factors (e.g., earthquakes, cave-in collapse); (ii) aggravating factors (e.g., floods, snowmelt and rainfalls; Zêzere et al. 1999).

Predisposing factors

Three topographic factors were used for this analysis (slope, aspect, curvature, stream network). The topographic factors were extracted based on high-precision SRTM DEM data. It provides a quasi-global representation of the Earth's surface at a medium spatial resolution (30–90 m). This data is obtained from Shuttle Radar Topography Mission (SRTM) and is available in website https://earthexplorer.usgs.gov/ with medium resolution 30 m/ cells of resolution.

Slope gradient is considered to as one of the main factors conditioning the triggering of landslides (Van Westen et al. 2008; Petley et al. 2005; Kuriakose et al. 2008). The value derived from the DTm is divided into five classes consistent with a 10° interval for each (> 10°) (10°–20°), (20°–30°) (30°–40°), and (< 40°) (Van Westen 2006; Petley et al. 2005; Kuriakose et al. 2008) (Fig. 6a). Slope aspect is considered as a influencing factor which controlled the landslides triggering (Pradhan and Lee 2010; Schlögel et al. 2018; Pourghasemi et al. 2012; Yan et al., 2020). Slope aspect is defined as the direction in which a slope is oriented and it relates to the degree of exposure to the sun. This factor also influences the plant cover, the daily temperature, and relative humidity ranges of a slope (Chen et al. 2019). For this purpose, the slope aspect map has been classified in 8 distinct classes (N, NE, E, SE, S, SW, W, and NW); the distribution of landslides related to slope aspect can be shown in Figure 6 b. Another factor that can be considered in landslide hazard analysis is topographic curvature. Indeed, slopes curvature profile characterizes the morphology of the topography and has a positive influence on the onset of landslides. The slope curvature influences the training and resistance stresses in a landslide in the direction of motion and controls the change in speed of mass motion flowing down the slope The value of the curvature can be either above, below, or equal to zero, representing the convex, concave, or flat shaped curvatures, respectively (Fig. 6c).

Geo-environmental and anthropogenic factors were involved in this analysis by a landcover spatial data. The land cover map was obtained from supervised classification of Landsat (Oli_8) and compared to the map developed by forestry services. This map of has been prepared and classified into four distinct categories (dense forest, sparse vegetation cover, pasture areas, and totally bare soil) (Fig. 6d). (Table 1).

Geological factors were split in three different spatial variables with (i) a lithological map; (ii) a characteristics of materials; and the (iii) structure with integration of faults. The lithological map was established by digitizing two geological maps (Mascara and Mohamadia maps with 1/50000 scale) (Dalloni 1936). The geological section contains geologic formations dating from Cretaceous to Plio-Quaternary. According to the friability of the rocks, these formations were classified into 4 categories and (crumbly rock, soft rock, competent rock, and very resistant rocks) (Fig. 6f). The characteristics of the material itself result from the bedrock, weathering may be weak or fractured, or different layers may have different strengths and rigidity. For this purpose, three geological factors were taken into account for this analysis. The structural map is based on fault lineaments extracted from the old geological maps, and drawn from the morpho-structural analysis using photo-interpretation of satellite images coupled with a shaded DEM. This data represents the distance to fault map was constructed by generating buffers along the fault lines. This distance was classed into 4 classes (0–250 m), (250–500 m), (500–1000 m), and (> 1000 m), more the area is located near the fault line, the risk of slipping is very likely (Fig. 6e).

Aggravating factors

Aggravating factors can depicted as factors s accentuating the possibility to have landslide occurrences without actually triggering the phenomena. For example, a series of earthquakes can accentuate the fragility of materials without triggering landslides, or the fact that rainfall is higher than the annual average for some areas will induce a greater sensitivity for intense rainfalls for some land. Four aggravating factors have been selected with (i) mean precipitation data; (ii) seismic activity; (iii) stream network; and (iv) anthropogenic influence.

In our study area, landslides are triggered mainly following rainfalls, which can be intense and sudden. Due to lack of daily rainfall data, we used an annual mean precipitation map, produced using rainfall data from three weather stations located around the study area. The selected period is 10 years (from 2004 to 2014). The map is obtained by applying the ordinary Kriging method. The final map was prepared and reclassified into four classes based on the annual average rainfall (380–410 mm), (410–440 mm), (440–470 mm), and (470–500 mm) (Fig. 6g).

An earthquake or series of earthquake can accentuate the slope instability by the inertial loading it imposes or by causing a loss of resistance of the materials of the slope (Hadji et al. 2016; Yang et al. 2017; Huang et al. 2017). The Beni-Chougrane region, as all areas of northern Algeria, is characterized by moderate seismic activity (Refas et al. 2019). Indeed, large earthquakes shook this area in 1967 and 1994 (Benouar et al. 1994; Bezzeghoud and Buforn 1999). Therefore, the seismic sources were extracted from the international database (ANSS), of which 6 large sources located in
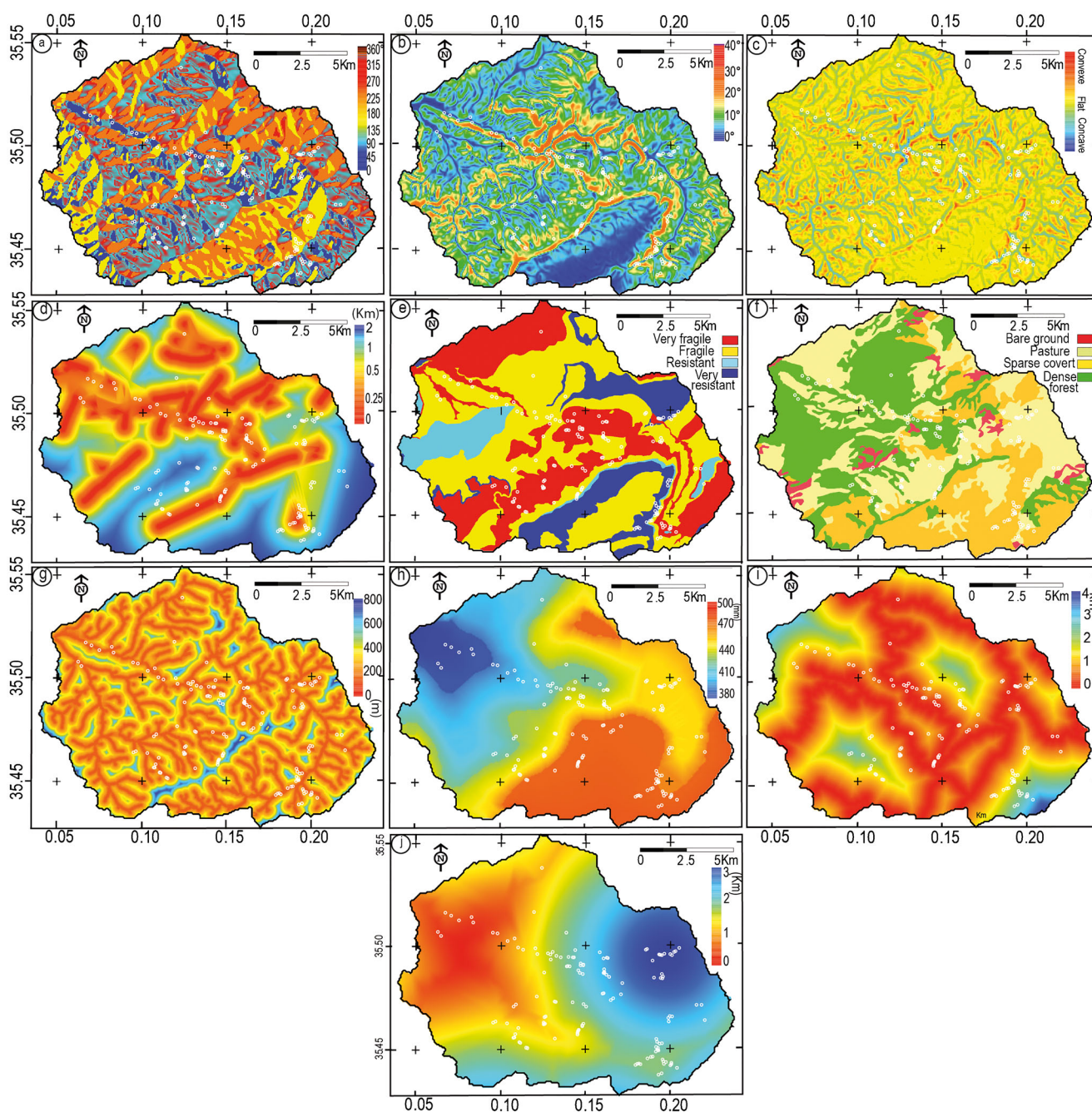
Fig. 6 Causal factors responsible for triggering landslide a: slope, b: aspect, c: curvature, d: tectonic fault, e: lithology, f: land cover, g: stream network, h:rainfall, i: road traffic and j: earthquakes. The white circles represent the spatial distribution of landslide

the vicinity of the Fergoug watershed. A buffer was applied around these sources. Based in this strategy, the prepared raster map was classified into 4 classes representing by distances (> 500 m), (500–1 km), (1–3 km), and (> 3 km) (Fig. 6h).Remote areas of seismic sources have a low probability of generating a landslide.

The distance to stream networks can a fundamental parameter controlling the landslide occurrences. We can then consider that the basal cutting of the banks can induce landslides

by foot failure. In the Fergoug watershed, three rivers cross it diagonally with lengths 24.9, 12.7, and 9.70 km respectively for Fergoug, Taghzout, and Hammam rivers. Moreover many tributaries spread out along the study area. Then, we extracted the water system from the SRTM-DTM, and buffers of a distance of 50 m were applied. The raster map was coded using a distance-based strategy. According to this distance, five classes have been highlighted: (< 50 m), (50–100 m), (100–150 m), (150–200 m), and (> 200 m) (Fig. 6i).

Human activities and road construction works (digging, excavation, and trenching) can be an important aggravating factor for landslide occurrences. The slope gradient can be artificially increased inducing a higher failure probability.

Beyond this increase in local slopes, many authors have shown along roadways the effect of traffic on landslide initiation (Shipway et al. 2015; Voumard et al. 2013; Jotic et al. 2018). Indeed, this road traffic can cause incessant vibrations that then affect the stability of the slope. To determine this effect, we mapped out all roads crossing the Fergoug area and then proceeded to apply buffers at random distances (500 m), (1 km), (2 km), and (> 2 km) (Fig. 6j). This strategy is based on the fact that the closer the area is to the road, the higher the probability of triggering a landslide.

Landslide susceptibility modeling

For each selected method, the procedure to compute landslide susceptibility map is the same with a confrontation of the events (i.e., landslides) with the factors. The reliability of each model used to produce susceptibility map is carried out through a classical procedure based on the computation of receiver operating characteristics (ROC) and the area under curve (AUC). The tests were performed by comparing known landslide location data with the landslide susceptibility map. To determine the reliability of three models of landslide susceptibility (FR, IVM, and RLM) applied in this study, we performed a check using the receiver operating characteristic curve, or ROC curve, which is graphical representation created by plotting the true positive rate (TPR) known as sensitivity against the false positive rate (FPR) known as specificity and this at various threshold settings (Pourghasemi et al. 2012). By tradition, the ROC curve is plotted using False Positive Rate on X-axis (shown in Eq. (6)) and True Positive Rate on Y-axis (shown in Eq. (7)):

$$X = \text{Specificity} = 1 - \left[\frac{TN}{TN + FP} \right] \tag{6}$$

$$Y = \text{Sensitivity} = \left[\frac{TN}{TP + FN} \right] \tag{7}$$

Where TP (True positive) is the number of landslide pixels correctly classified in the landslide class, and TN (True negative) is the total number of non-landslide pixels correctly classified in the non-landslide class of ground. FP (false positive) is the number of landslide pixels classified in the non-landslide class; FN (False negative) is the non-slip pixels classified in the class of landslides (Xu et al., 2012).

Usually, AUC curves range from 0.5 to 1.0. The model with a higher AUC is considered the best. If the area under the ROC curve (AUC) is close to 1, the test result is excellent (Hong et al., 2016). On the other hand, if the model does not predict well, then this value will be close to 0.5. Related to test value, it can be divided in five class, the value ranges from 0.50 to 0.60 (poor), 0.60–0.70 (average), 0.70–0.80 (good), 0.80–0.90 (very good), and 0.90–1.00 (excellent) (Pourghasemi et al. 2012).

Results and discussion

Results are analyzed in three steps with (i) analysis of predisposing factors, (ii) analysis of aggravating factor, and (iii) analysis of final maps. Each part is discussed. By this way, we explore and analyze simultaneously the influence of each predictive factor and how each model how each model behaves in relation to the data.

The results in Table 2 show that the values obtained by the information value model (IVM) are almost consistent with the values of the frequency ratio (FR). The statistical correlation between landslides and their independent factors was determined by the multiple linear regression (MLR) model. Based on constant values of regression coefficients, the landslide occurrence predicting equation was obtained as follows:

$$LSI\ (MLR) = 0.692 - 0.194\ (Roads) - 0.086\ (Vegetation) \tag{8}$$
$$+ 0.175\ (faults) + 0.085\ (exposition)$$
$$+ 0.138\ (Slope) - 0.013\ (Lithology) - 0.048\ (Rainfall)$$
$$+ 0.208\ (Stream\ network) + 0.189\ (Earthquakes)$$
$$+ 0.027\ (Curvature\ topography).$$

Analysis of predisposing factors

Slope aspect bounded for (NE, E, SE, and S) has rational correlation with landslide occurrence; however, the higher value (FR = 5.87) marked the Northern slope exposition (Fig. 6a). This can be explained by the morphological disposition of the mountainous chain. Indeed, Beni-Chougrane Mountains are oriented ENE-WSW and the ridges divide slopes into two categories, Northern and Southern slopes. These mountains are anticlines limb with steep slopes. These anticlines are overturned to the south; therefore, the north-facing slopes are larger than the southern facing, and are characterized by a significant number of landslides, the north-facing slopes are wetter than those facing south. Among the slope categories, high landslide frequency ratio is observed in slope smaller than 10° (FR = 2.09). This is due to the total lack of sufficient plant cover to protect these lands. Knowing that Fergoug forest is located in the Western part and occupied the higher altitudes. In addition, these lands are the result of

Table 2 A spatial relationship between listed landslides and conditioning factors in the study area. For abbreviations, FR = frequency ratio, IVM = information value model and MLR = multiple linear regression

Factors/CLASS	N0. of pixels	Pixels domain	Pixels domain %	Landslide occurrence (N)	Landslide occurrence %	FR	IVM	MRL
Aspect								0.085
NE	15390	15390	9.13	393	3.53	0.39	− 1.37	−
E	31080	15690	9.31	607	5.45	0.59	− 0.77	−
SE	47260	16180	9.60	585	5.25	0.55	− 0.87	−
S	69950	22690	13.46	407	3.65	0.27	− 1.88	−
SW	92740	22790	13.52	32	0.29	0.02	− 5.56	−
W	117830	25090	14.88	91	0.82	0.05	− 4.19	−
NW	146910	29080	17.25	611	5.48	0.32	− 1.65	−
N	168600	21690	12.86	8416	75.53	5.87	2.55	−
Slope								0.138
< 10	55970	55970	33.20	7730	69.38	2.09	1.06	−
10–20	140920	84950	50.39	1280	11.49	0.23	− 2.13	−
20–30	163850	22930	13.60	1672	15.01	1.10	0.14	−
30–40	167800	3950	2.34	362	3.25	1.39	0.47	−
> 50	168600	800	0.47	98	0.88	1.85	0.89	−
Faults								0.175
0.25	35660	35660	21.15	7987	71.68	3.39	1.76	−
0.50	94720	59060	35.03	1538	13.80	0.39	-1.34	−
1	149290	54570	32.37	1523	13.67	0.42	-1.24	−
2	168600	19310	11.45	94	0.84	0.07	-3.76	−
Lithology								0.013
Crumbly rocks	24640	24640	14.61	2988	26.82	1.83	0.88	−
Soft rocks	102040	12450	7.38	1448	13	1.76	0.82	−
Competent rocks	156150	54110	32.09	5743	51.54	1.61	0.64	−
Resistant rocks	168600	77400	45.91	963	8.64	0.19	− 2.64	−
Rainfall (mm)								−
								0.0-48
380–410	33920	33920	20.12	2981	26.75	1.33	− 0.18	−
410–440	77850	43930	26.06	1591	14.28	0.55	− 0.89	−
440–470	127250	49400	29.30	3186	28.59	0.98	− 0.46	−
470–500	168600	41350	24.53	3384	30.37	1.24	0.13	−
Stream network (m)								0.208
< 0.1	32675	32675	19.38	7435	66.73	3.44	1.56	−
0.1–0.25	71886	39211	23.26	2164	19.42	0.84	0.89	−
0.25–0.5	113175	41289	24.49	983	8.82	0.36	3.75	−
> 0.5	168600	55425	32.87	560	5.03	0.15	− 2.57	−
Roads (Km)			0					− 0.19
< 0.5	16.99	16990	10.08	1978	17.75	1.76	0.82	−
0.5–1	54.85	54850	32.53	5017	45.03	1.38	0.47	−
1–2	57.14	57140	33.89	2999	26.92	0.79	− 0.33	−
> 2	39.62	39620	23.50	1148	10.30	0.44	− 1.19	−
Earthquake (KM)								0.189
< 1	6490	6490	3.85	2198	19.73	5.12	2.36	−
1–2	111780	105290	62.45	8507	76.35	1.22	0.29	−
> 3	168600	56820	33.70	437	3.92	0.12	− 3.10	−
Landcover								

Table 2 (continued)

Factors/CLASS	N0. of pixels	Pixels domain	Pixels domain %	Landslide occurrence (N)	Landslide occurrence %	FR	IVM	MRL
								−
								0.0-86
Permanent vegetal cover	168600	59510	35.30	11	0.10	0	− 8.48	−
Temporary Vegetal cover	44100	44100	26.16	1067	9.58	0.37	− 1.45	−
Pastures	103400	59300	35.17	6496	58.30	1.66	0.73	−
Bare soils	109090	5690	3.37	3568	32.02	9.49	3.25	−
Curvature								0.027
Concave	37505	37505	22.24	396	3.55	0.16	− 2.65	−
Flat	129154	91649	54.36	592	5.31	0.10	− 3.35	−
Convex	168600	39446	23.40	10154	91.13	3.90	1.96	−

anarchic exploitation by farmers. The frequency ratio is less than 1, indicating a lower probability of triggering a landslide in the slope class ranged between 10° and 20°. However, the areas which correspond to slopes ranging from 20° and higher than 50° are exposed to very significant chemical and physical alteration processes and there are characterized by higher value (> 1). This is due to the rising of shear stress in steep slopes under the gravity effect (Fig. 6b).

The relationship between curvature and landslide indicates that they generally occur in or near concave slopes where FR values are significant and are greater than 3. Our results show also that the FR values are more significant in concave slope and less significant (< 1) in the flat slope (Fig. 6c).

The results obtained using the FR model show that regions most sensitive to landslides are distributed in areas situated near faults (Fig. 6d). FR value of 3.39 is obtained for areas closer to the fault line which are characterized by a distance not exceeding to 0.25 km. These areas represent 71.68 % of landslide occurrence. Our results show also that the less important FR is obtained for area located far from the fault line. Indeed, the FR ratio is −1.34, − 1.4, and − 3.76 respectively for zones situated between 0.5 and 1 km, between 1 and 2 km, and beyond 2 km.

Values of FR = 1.83 and are attributed to zones which is characterized by a crumbly rock in particular marls and clays. Due to the presence of clay and marl particles exposed to water, these reach very quickly the liquidity limit and the lands slide easily. Resistant rocks are characterized by very less value (FR = 0.19) (Fig. 6e).

The denuded areas are represented by significant value FR = 9.49. However, FR is less than 1 in areas characterized by permanent forest cover (Fig. 6f).

The results shown in Table 2 show that values obtained by the information value model (IVM) are almost consistent with the values of the frequency ratio (FR). In fact, the most significant values are those which correspond to approximate areas with faults. IVM values are also important in areas characterized by IVM values of 1.06, 0.88, and 3.25 respectively for steep slopes, crumbly rocks, and bare soil.

According to the equation (Eq. (8)) obtained, 6 parameters statistically significant; however, 3 parameters generally considered as less important. For faults, the regression coefficient Cr have positive value respectively (Cr = 0.175). Indeed, this topographic factor is considered to be one of the determining factors in the triggering of landslides, and represents the most effective parameter in terms of landslides occurrence. This shows their decisive role in promoting landslide activities.

Slopes, curvature, exposure, and lithology have proven to be moderately important in the current context with low values respectively 0.138, 0.085, 0.027, and 0.013.

Coefficients related to the vegetation and roads were recorded with negative Cr values (− 0.086 and − 0.019), which proves that these factors are less important to promote landslide activities.

Analysis of aggravating factors

Our results show that 66.73% of landslide occurrence is reported to areas which correspond to distances of river ranges < 100 m. In these zones, the FR is marked by a higher value (FR = 3.44). The values of the FR become lower as we move away from rivers. FR is 0.84, 0.36, and 0.15 respectively for areas between (100–250 m), (250–500 m), and beyond 500 m (Fig. 6g).

This indicates a good correlation between these hydrological parameters and landslide occurrence. The erosion exerted in the meanders of a river continuously digs deep in the bed of the river, undermining and weakening the banks, and causing their collapse. This is caused by a breakage of the stopper of the foot and thus leads to undermining of the banks. To this

end, areas closer to rivers (< 100 m) have a stronger relationship with landslides. Presumably, areas characterized by a dense hydrographic network have also, a high probability of landslides occurrence (Karim et al. 2019).

Our results show that it exists a very important relationship between annual and daily precipitation and the occurrence of landslides. This indicates that landslides correlate very well with high rainfall values (FR = 1.24) (Fig. 6h). This confirms that precipitation, especially rains, is the trigger for landslide. It has been found that cumulative precipitation of 10 to 30 days is mainly associated not only with the triggering of landslides but also with their reactivation.

In the case of our study area, this is can easily observed in the landslides affecting the Mohamadia road (Fig. 3a, b). Indeed each winter, the municipality implements remediation work after the damage caused by the landslide and this to ensure the continuity of road traffic. In the case of our study area, there is a positive dependent relationship between altitude and precipitation, landslides generally occur in high altitude areas surrounding in particular the Sidi Daho syncline (Fig. 1b). It should be noted that torrential rains are considered to be the main trigger for landslides in the Fergoug watershed. Several landslides are triggered during the wet seasons, especially in winter. The relationship between roads proximity and landslides indicates that it occurred generally near roads at distances smaller than 500 m (Table 2) where FR = 1.76. Several roads are typically affected by this phenomenon (Fig. 3 and Fig. 4d). Indeed, in the case our study, the degradation of the roads begins with a simple cracking due to the removal of a stabilizing abutment in downstream, and then these cracks develop to evolve to more or less spaced openings leading to the sliding of the entire facade (Fig. 6i). In most time, this degradation is due to the anarchic construction of roads by increasing the gradient of slope without thinking on the stability measures (Solaimani et al. 2013) (Fig. 6i) (Fig. 3d). In many parts of the world, earthquakes are frequently accompanied by gravitational instabilities, particularly landslides and rock fall (Marc et al. 2015; Li et al. 2016; Zaagane et al. 2016; Roback et al. 2018; Veh et al., 2019). During the twentieth century, nearly 80 earthquakes caused between 100.000 to 1.000.000 landslides that claimed tens of thousands of lives (Keefer 1984). The zones characterized by an important seismic activity are also the seat of several landslides. Indeed in our study, FR = 5.12 value characterizes all areas situated less than 1 km from the seismic source (Fig. 6j).

FR values decrease in areas far from seismic sources where landslides are rare.

Our results show that IVM values are very important for hydrographic networks, seismic sources, and roads. Indeed IVM values are 1.56 for areas located near river lines with distance not exceed at 0.1 km to river. IVM value (IVM = 5.12) characterized area situated in circle that the radius is less than 1 km. For the anthropogenic factors, the IVM value is more and characterized all areas situated near road with distance not exceed at 0.5 km.

For the MRL model, the results in Table 2 shown that the coefficient linked to the hydrographic network has very strong dependence (Cr = 0.208). This indicates that the distance from the river corresponds to a high positive Cr which confirms a higher dependence between the banks and the landslides. Earthquakes have a clearly positive coefficient (Cr = 0.189). Indeed, landslides are largely triggered by earthquakes all over the world which can greatly increase the destructive impact of earthquakes especially in mountainous regions. These triggered landslides represent a significant proportion of the total earthquake damage due to the destruction of buildings and the impacts of landslides on lifelines and roads traffics that can been used in case of the rescue efforts.

Rainfall effects are more represented with MLR models. Indeed, Cr values are negative where Cr = − 0.048. The spatial distribution of rainfall has a secondary effect on the triggering of landslides; however, it should be noted that the rainwater joins the main rivers along the slopes, and it is the flood waters which are responsible in triggering landslides.

Analysis of final maps

The LSI landslide calculated using the FR and IVM model was summarized in all factor classes as shown in the equation (Eq. (2) and Eq. (5)), then we ranked the LSI values at an equal interval. The high LSI value is closely related to the total combination of factors controlling landslides. We then produced a raster map by assigning the value FR to each class of factors. We proceeded in the same way to establish the LSI map using the IVM model.

To predict the possibility of landslide, the probability was calculated from Eq. (8) then converted to raster format (Table 2).

Figure 7 shows the raster maps of LSI (FR), LSI (IVM), and LSI (MLR). These maps are represented by values ranging from 0.0245 to 1.931, and between − 0.004 and 89.25 respectively for the FR and IVM.

The values of the susceptibility map calculated by the MLR model show a range from 3.44 to 122.16. These values ranges were divided into five classes of susceptibility to landslides of equal intervals for the three models Very Low (VL), Low (L), Middle (M), High (H), and Very High) (VH) (Fig. 7).

The map produced using FR model shows a very important zone characterized by Very high landslide susceptibility located especially in the central zone of the Fergoug watershed especially around the Fergoug River (Fig. 7a). MLR model shows almost the same characteristic of susceptibility zone; however, the very high is less significantly compared to the LSI_FR map (Fig. 7b).

The very high and high susceptibility classes are well represented in the two maps produced by the FR and IVM models. Indeed, the very high susceptibility class presents a
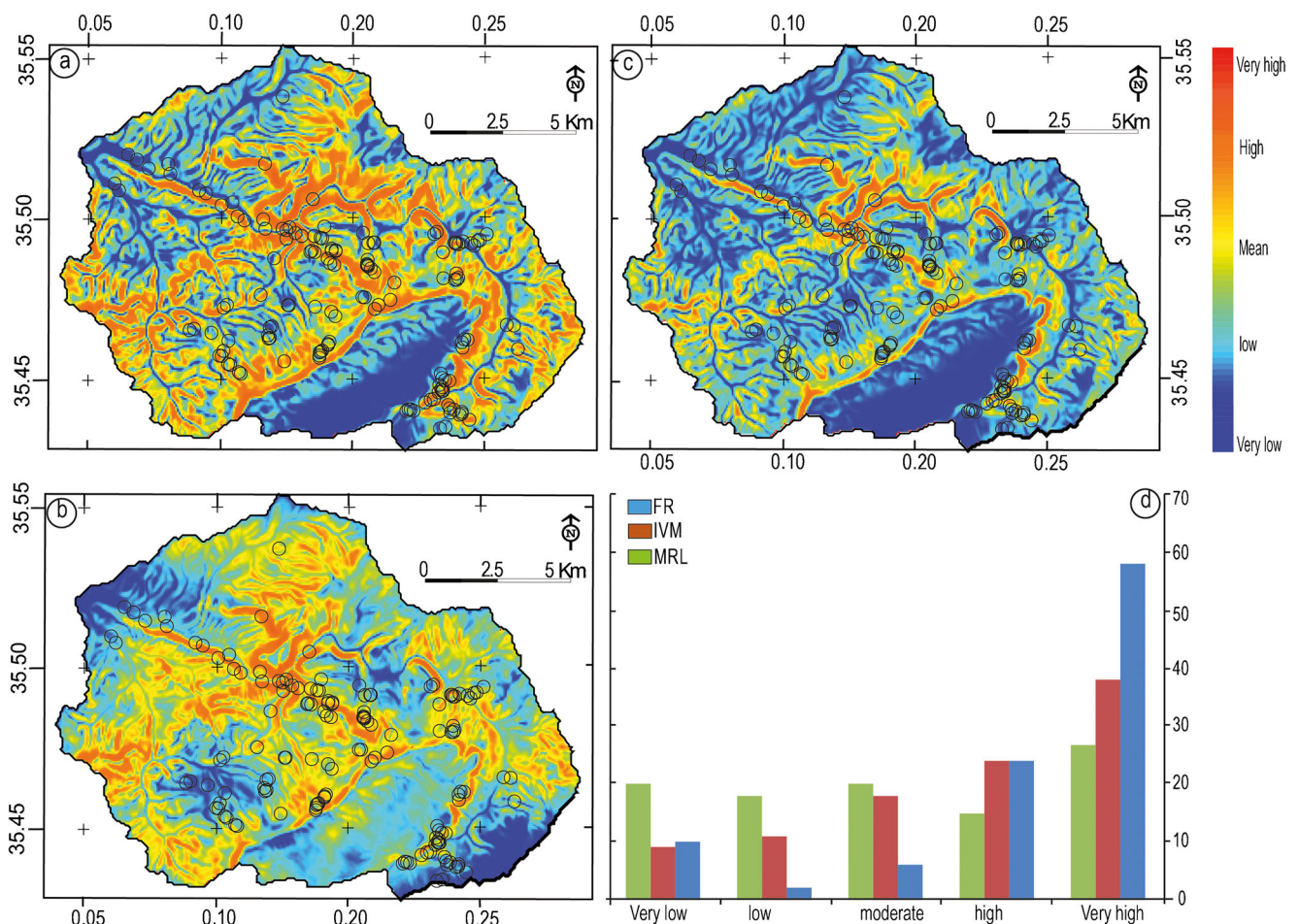
Fig. 7 Susceptibility maps produced using three models a: Frequency Ratio (FR) b: Information Value Model (IVM) and c: Multiple Linear Regression (MLR). The histogram in (d) represent the porcentage of each susceptibility class relating to (FR), (IVM) and (MLR) models

percentage of 58% for the Fr model and 47% for the IVM model (Fig. 7d). Although this percentage is less significant for the MLR model and is characterized by only 27% of the total area. However, the four classes are almost equal with percentages not exceeding 26% (Fig. 7d).

For the MLR model, the map produced shows the biggest zone represented by the Very low susceptibility class related to FR and IVM models (Fig. 7c). Indeed, 20% of the total area is represented by very low susceptibility; however, it is almost 10% for two models cited above.

For three models used in this study, the Fergoug River is considered as a very active in which almost the majority of the listed landslides are located along this zone.

The susceptibility map produced by the three models FR, IVM, and MLR shows very good spatial similarity. Indeed, the highest susceptibility classes are very important, and are listed on slopes greater than 40°, and along the main line of the river. The greatest probability is reported in this corridor located between the Mohamadia road and the Fergoug River. Towards the south of this watershed, the high density of landslides is located on both

sides of the perched syncline of Sidi Daho where two factors have been combined. This combination represents the steep slope associated with soft geological rocks represented mainly by Miocene marls. This observation proves that the good correlation between conditional factors such as slope and hydrographic network as well as a landslide was illustrated by the three models (FR, IVM, and MLR).

Validation

Choosing an adequate model to map landslide susceptibility (LSM) and determining its accuracy is an important aspect of research on landslide sensitivity. Checking landslide susceptibility maps is very important. Consequently, three commonly used statistical parameters, the receiver operating characteristic curve (ROC) and the area under the curve (AUC), the standard error and the 95% confidence interval are introduced to check the susceptibility maps of landslides. AUC and ROC curves have also been developed using the Excel-based (Xstalt) extension (Lee and Pradhan 2007; Pourghasemi et al. 2012).
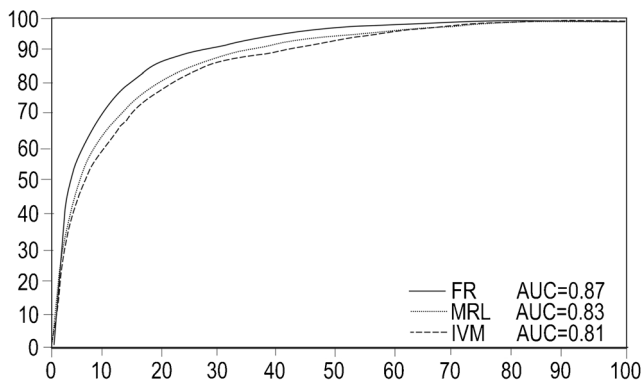
Fig. 8 Area under curve (AUC) of the ROC curve for the landslide susceptibility map produced by FR, IVM and MLR models

The results show that the FR, IVM, and MLR models used in this study give satisfactory results and show a very good precision in the prediction of the landslides susceptibility in the Fergoug area. Indeed, the AUC value is greater than 0.80 which means that the rate curve contains more than 80% of landslides in the three models (Fig. 8).

Results show that the FR model acquired the highest AUC value (0.87), followed by the IVM model (0.83) and

MLR model (0.81). The highly susceptible area with the prediction rate curve recognized by the FR model also includes more than 87 % of landslides, which illustrates that the precision of the FR model is the highest and that the FR model is the best model that can been used in this study.

It appears from this study, that during torrential rains, an intense runoff develops in the region of Fergoug. The tributaries discharge a large quantity of water and solid matter (soils, mixture of blocks and gravel uprooted upstream) to the main stream of Fergoug (Fig. 9a). Given the morphological aspect of this area, the materials transported by the floodwaters permanently erode the river bed. This erosion phenomenon occurs in two ways:

(i) A vertical erosion causing a deepening of the river bed and thus leads to an increase in the gradient of slope release of forces thus leading to mass movements towards the bed of the river (Fig. 9b, c).

(ii) A horizontal erosion resulting in the meanders erosion of this river leading to destabilize the slope (Fig. 9a). When
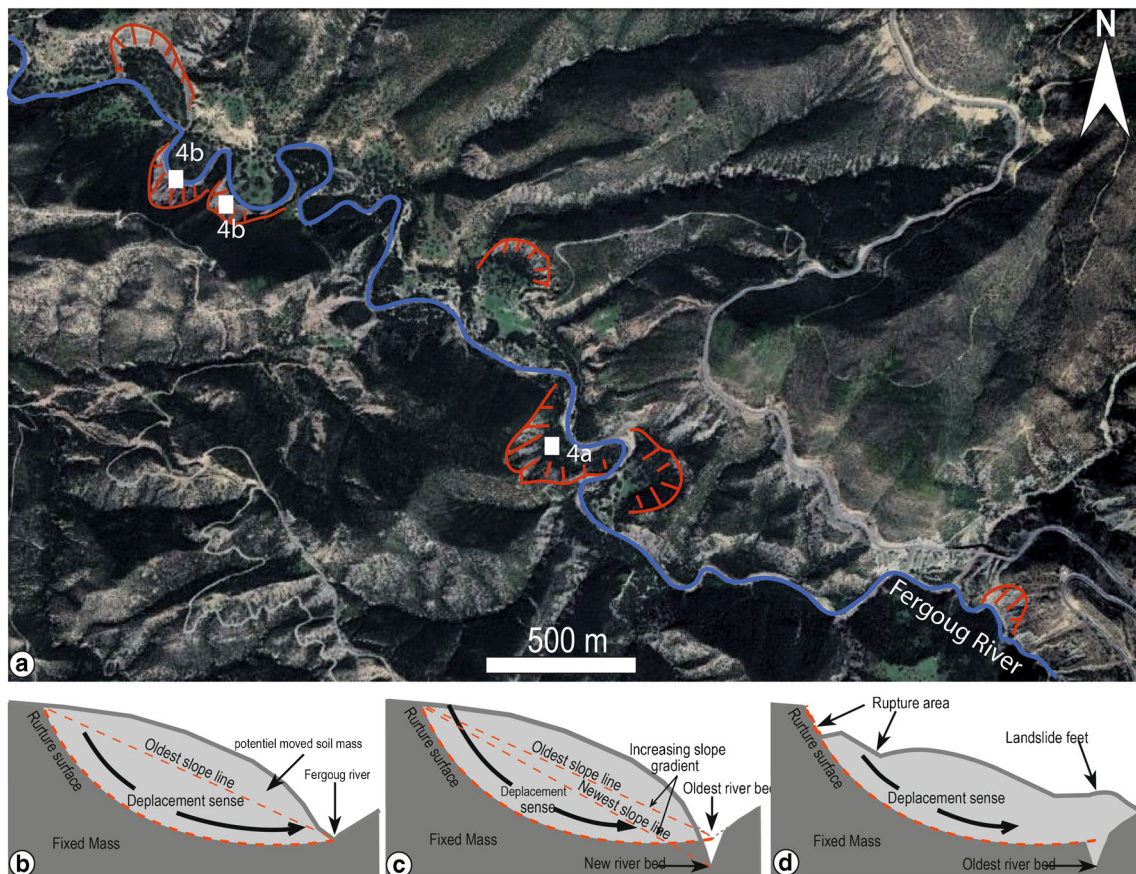

Fig. 9 Image showing the relationship between the Fergoug river and thelandslide triggering, a: the disposal of landslide along the river, especially in the meanders causing locally the change of the streamcourse b: scheme showing the initial stage in a failure slope, c: the deepening of the Wadi bed leading to the increase of the slope gradient,d: the triggering of landslides under the soil weight effect leading to the filling of the river bed by the mobilized land. For the symbols 4a, 4b please see the figure 4

the soils are slipped, this movement causes the widening of this river on the one hand and the modification of the flow of the fluvial network on the other hand (Fig. 9d). Along the Fergoug River, all these erosion products are transported to the Fergoug dam thus leading to its silting. This dam works with 5% of its total capacity. As a result, over 70% of the total surface area of citrus fields irrigated from dam is currently dry. Consequently, it is a real desperation for the local population that all of their economic activity is based heavily on the exploitation of water from the dam.

Conclusion

Like all areas of northern Algeria, the Fergoug watershed has strongly affected by landslides phenomenon. Indeed, during our trip field, we noticed that several infrastructures, such as roads, rivers and dams, even bridges, and houses have been affected by this phenomenon. It seems that many factors acted together on the slopes and leading to the triggering of landslides. In the case of our study area, landslides are mainly due to factors classing into two types: (i) predisposing factors including aspect, slope, the curvature, faults, soft geological rocks, land cover, and (ii) aggravating factors represented by aggressive precipitation, earthquakes, stream network and roads. Two research steps were followed in this process. Firstly, the realization of the hazard maps was carried out by applying the FR, IVM, and MLR models chosen for their performance and their simplicity, then, the results obtained were tested using AUC curve These tests show that our results show very good accuracy for all three models. Indeed, our results reveal that the frequency ratio model (87%), the IVM model (83), and the MLR models (81%) have been highly accurate and can be classified in the category of very good precision (> 80). Despite its simplicity, the FR model shows more precision than IVM and MLR models.

In the FR model, the biggest class of landslide susceptibility is represented by high to very high class, accounting for more than 80% of the area, compared to 60% in the IVM model and 41% for MLR.

The multiple linear regression equation allows us to conclude that landslide causal factors (distance from faults and stream network, curvature, slope and earthquakes) have a significant influence on landslides.

The landslide susceptibility maps obtained as part of this study also showed that an area with significant landslide risk was located in the central part of the Fergoug watershed. The results also show that the lands most likely to cause this type of instability are spread around the Fergoug River bed.

The road that connects the Mascara town and the Mohamadia is used by thousands of car drivers every month.

This road has a high susceptibility to landslides, while more than 5% of the inhabitants are distributed along the edges of this road and on extremely sensitive lands. To this end, the models used in this study have shown that susceptibility mapping is an essential tool for delimiting areas prone to landslides. These maps can be considered an important piece of information for decision makers. They have to be the basis for future plan decision and they are in line with the government's desire to improve landslide hazard documents by being easy to implement and easily understood by practitioners.

Declarations

Conflict of interest   The authors declare that they have no competing interests.

References

Arora M, Das Gupta A, Gupta R (2004) An artificial neural network approach for landslide hazard zonation in the Bhagirathi (Ganga) Valley, Himalaya. Int J Remote Sens 25:559–572

Balsubramani K, Kumaraswamy K (2013) Application of geospatial technology andinformation value technique in landslide hazard zonation mapping: a case study of Giri Valley, Himachal Pradesh. Disaster Advances 6:38–47

Benouar D, Aoudia A, Maouche S, Meghraoui M (1994) The 18 August 1994 Mascara (Algeria) earthquake — a quick-lookreport. Terra Nova 6:634–637

Bezzeghoud M, Buforn ER (1999) Source parameters of the 1992 Melilla (Spain, Mw: 4.8), Alhoceima (Morocco, Mw: 5.8) and 1994 Mascara (Algeria, Mw: 5.7) earthquakes and seismotectonics implications, Bulletin of Seismologic Society of America. 89 359–372

Caiyan WU, Jianping Q (2009) Relationship between landslides and lithology in the Three Gorges Reservoir area based on GIS and Information Value Model. Higher Education Press and Springer New York 4(2):165–170

Cánovas JB, Stoffel M, Martín-Duque JF, orona C, Lucía A, Bodoque JM, Montgomery DR (2017) Gully evolution and geomorphic adjustments of badlands to reforestation. Scientific reports 7(1):1-8.

Champatiray P (2000) Personalization of cost effective methodology for landslide hazard zonation using RS and GIS: IIRS initiative. In: Roy P, Van Westen C, Jha V, Lakhera R (eds) Natural disasters and their mitigation; remote sensing and geographical information system perspectives. Indian Institute of Remote Sensing, Dehradun, India, pp 95–101

Champatiray P, Dimri S, Lakhera R, Sati S (2007) Fuzzy based methods for landslide hazard assessment in active seismic zone of Himalaya. Landslides 4:101–110

Chattoraj J, Gendelman O, Ciamarra MP, Procaccia I (2019) Oscillatory instabilities in frictional granular matter. Phys Rev Lett 123(9): 098003

Chen W, Shahabi H, Shirzadi A, Hong H, Akgun A, Tian Y, Liu J, Li A-XZS (2019) Novel hybrid artificial intelligence approach of bivariate statistical-methods-based kernel logistic regression classifier for landslide susceptibility modeling. Bull Eng Geol Environ 78(6): 4397–4419

Corominas J, van Westen C, Frattini P, Cascini L, Malet JP, Fotopoulou Catani F, Van Den Eeckhaut M, Mavrouli O, Agliardi F, Pitilakis K, Winter MG, Pastor M, Ferlisi S, Tofani V, Hervás J, Smith JT (2014) Recommendations for the quantitative analysis of landslide risk. Bull Eng Geol Environ 73(2):209–263

Cui Y, Cheng D, Choi CE, Jin W, Lei Y, Kargel JS (2019) The cost of rapid and haphazard urbanization: lessons learned from the Freetown landslide disaster. Landslides 16(6):1167–1176

Dalloni M (1936) carte géologique de Mascara, service de la carte géologique de l'Algérie, n°: 212

Dikau R (1999) The recognition of landslides. In Floods and Landslides: Integrated Risk Assessment (pp. 39-44). Springer, Berlin, Heidelberg

Erzin Y, Cetin T (2013) The prediction of the critical factor of safety of homogeneous finite slopes using neural networks and multiple regressions. Comput Geosci 51:305–313

Felicísimo ÁM, Cuartero A, Remondo J, Quirós E (2013) Mapping landslide susceptibility with logistic regression, multiple adaptive regression splines, classification and regression trees, and maximum entropy methods: a comparative study. Landslides 10(2):175–189

Frattini P, Crosta GB, Rossini M, Allievi J (2018) Activity and kinematic behaviour of deep-seated landslides from PS-InSAR displacement rate measurements. Landslides 15(6):1053–1070

Ghimire M (2011) Landslide occurrence and its relation with terrain factors in the Siwalik Hills, Nepal: case study of susceptibility assessment in three basins. Nat Hazards 56(1):299–320

Gholami M, Ghachkanlu EN, Khosravi K, Pirasteh S (2019) Landslide prediction capability by comparison of frequency ratio, fuzzy gamma and landslide index method. J Earth System Science 128(2):42

Guzzetti F, Mondini AC, Cardinali M, Fiorucci F, Santangelo M, Chang KT (2012) Landslide inventory maps: new tools for an old problem. Earth Sci Rev 112(1-2):42–66

Gzzetti F, Reichenbach P, Ardizzone F, Cardinali M, Galli M (2006) Estimating the quality of landslide susceptibility models. Geomorphology 81(1-2):166–184

Hadji R, Chouabi A, Gadri L, Raïs K, Hamed Y, Boumazbeur A (2016) Application of linear indexing model and GIS techniques for the slope movement susceptibility modeling in Bousselam upstream basin, Northeast Algeria. Arab J Geosci 9(3):192

Hong H, Pourghasemi HR, Pourtaghi ZS (2016) Landslide susceptibility assessment in Lianhua County (China): a comparison between a random forest data mining technique and bivariate and multivariate statistical models. Geomorphology, 259, 105-118.

Huang MH, Fielding EJ, Liang C, Milillo P, Bekaert D, Dreger D, Salzer J (2017) Coseismic deformation and triggered landslides of the 2016 Mw 6.2 Amatrice earthquake in Italy. Geophys Res Lett 44(3): 1266–1274

Hungr O (2018) Some methods of landslide hazard intensity mapping. In Landslide risk assessment (pp. 215-226). Routledge

Javier and Kumar. (2019) Frequency ratio landslide susceptibility estimation in a tropical mountain region, The International Archives of the Photogrammetry, Remote Sensing and Spatial Information Sciences, Volume XLII-3/W8, 2019 Gi4DM 2019 – GeoInformation for Disaster Management, 3–6 September 2019, Prague, Czech

Jotic M, Vujanic V, Mitrovic P, Jelisavac B, Zarkovic Z (2018) Specific features of the landslide "Bracin" at the chainage km: 750+ 500 of E-75 international road through Yugoslavia. In Landslides (pp. 589-596)

Kanungo D, Arrora M, Sarkar S, Gupta R (2009) Landslide Susceptibility Zonation (LSZ) mapping — a review. J South Asia Disaster Studies 2:81–105

Karim Z, Hadji R, Hamed Y (2019) GIS-based approaches for the landslide susceptibility prediction in Setif Region (NE Algeria). Geotech Geol Eng 37(1):359–374

Keefer DK (1984) Landslides caused by earthquakes. Bull Seismol Soc Am **95**:406–421

Kuriakose SL, Jetten VG, Van Westen CJ, Sankar G, Van Beek LPH (2008) Pore water pressure as a trigger of shallow landslides in the Western Ghats of Kerala, India: some preliminary observations from an experimental watershed. Phys Geogr 29(4):374–386

Lari S, Frattini P, Crosta GB (2014) A probabilistic approach for landslide hazard analysis. Eng Geol 182:3–14

Lee S, Pradhan B (2007) Landslide hazard mapping at Selangor, Malaysia using frequency ratio and logistic regression models. Landslides 4(1):33–41

Lee S, Sambath T (2006) Landslide susceptibility mapping in the Damrei Romel area, Cambodia using frequency ratio and logistic regression models. Environ Geol 50(6):847–855

Li G, West AJ, Densmore AL, Hammond DE, Jin Z, Zhang F et al (2016) Connectivity of earthquake-triggered landslides with the fluvial network: Implications for landslide sediment transport after the 2008 Wenchuan earthquake. J Geophys Res Earth Surf 121(4):703–724

Liu JG, Mason PJ, Clerici N, Chen S, Davis A, Miao F, Deng H, Liang L (2004) Landslide hazard assessment in the Three Gorges area of the Yangtze river using ASTER imagery: Zigui–Badong. Geomorphology 61(1-2):171–187

Mahdadi F, Boumezbeur A, Hadji R, Kanungo DP, Zahri F (2018) GIS-based landslide susceptibility assessment using statistical models: a case study from Souk Ahras province, NE Algeria. Arab J Geosci 11(17):476

Manchar N, Benabbas C, Hadji R, Bouaicha F, Grecu F (2018) Landslide susceptibility assessment in Constantine Region (NE Algeria) by means of statistical models. Studia Geotechnica et Mechanica 40(3):208–219

Marc O, Hovius N, Meunier P, Uchida T, Hayashi S (2015) Transient changes of landslide rates after earthquakes. Geology 43(10):883–886

Mekerta B, Semcha A, Rahmani F, Troalen JP (2008) Erosion spécifique et caractérisation de la résistance au cisaillement des sédiments du barrage de Fergoug. Xèmes Journées Nationales Génie Civil–Génie Côtier 1:14–15

Mosavi A, Ozturk P, Chau KW (2018) Flood prediction using machine learning models: Literature review. Water 10(11):1536

Mousavi SZ, Kavian A, Soleimani K, Mousavi SR, Shirzadi A (2011) GIS-based spatial prediction of landslide susceptibility using logistic regression model. Geomatics, Natural Hazards and Risk 2(1):33–50

Mugagga F, Kakembo V, Buyinza M (2012) Land use changes on the slopes of Mount Elgon and the implications for the occurrence of landslides. Catena 90:39–46

Nichol J, Wong MS (2005) Satellite remote sensing for detailed landslide inventories using change detection and image fusion. Int J Remote Sens 26(9):1913–1926

Nsengiyumva JB, Luo G, Amanambu AC, Mind'je R, Habiyaremye G, Karamage F, Ochege FU, Mupenzi C (2019) Comparing probabilistic and statistical methods in landslide susceptibility modeling in Rwanda/Centre-Eastern Africa. Sci Total Environ 659:1457–1472

Onagh M, Kumra VK, Rai PK (2012) Landslide susceptibility mapping in a part of Uttarkashi district (India) by multiple linear regression method. Int J Geol, Earth Environ Sci 2(2):102–120

Palucis MC, Ulizio TP, Fuller B, Lamb MP (2018) Flow resistance, sediment transport, and bedform development in a steep gravel-bedded river flume. Geomorphology 320:111–126

Park S, Choi C, Kim B, Kim J (2013) Landslide susceptibility mapping using frequency ratio, analytic hierarchy process, logistic regression, and artificial neural network methods at the Inje area, Korea. Environ Earth Sci 68(5):1443–1464

Pasang S, and Kubíček P (2018) Information value model based landslide susceptibility mapping at Phuentsholing, Bhutan. In Proceedings of the 21st AGILE Conference, Lund, Sweden (pp. 12-15).

Passang S, Kubíček P (2018) Information value model based landslide susceptibility mapping at Phuentsholing. Bhutan, AGILE

Pereira S, Zezere J, Bateira C (2012) Assessing predictive capacity and conditional independence of landslide predisposing factors for shallow landslide susceptibility models. Nat Hazards Earth Syst Sci 12: 979–988

Petley DN, Higuchi T, Petley DJ, Bulmer MH, Carey J (2005) Development of progressive landslide failure in cohesive materials. Geology 33(3):201–204

Pourghasemi HR, Mohammady M, Pradhan B (2012) Landslide susceptibility mapping using index of entropy and conditional probability models in GIS: Safarood Basin, Iran. Catena 97:71–84

Pradhan B (2013) A comparative study on the predictive ability of the decision tree, support vector machine and neuro-fuzzy models in landslide susceptibility mapping using GIS. Comput Geosci 51: 350–365

Pradhan B, Lee S (2010) Landslide susceptibility assessment and factor effect analysis: back propagation artificial neural networks and their comparison with frequency ratio and bivariate logistic regression modeling. Environ Model Softw 25(6):747–759

Refas S, Safa A, Zaagane M, Souidi Z, Hamimed A (2019) Evaluation of seismic hazard using tectonic fault data: case of Beni-Chougrane Mountains (Western Algeria). Min Sci 26

Reichenbach P, Rossi M, Malamud BD, Mihir M, Guzzetti F (2018) A review of statistically-based landslide susceptibility models. *Earth-Science Reviews*, *180*, 60-91.

Roback K, Clark MK, West AJ, Zekkos D, Li G, Gallen SF, Chamlagain D, Godt JW (2018) The size, distribution, and mobility of landslides caused by the 2015 Mw7. 8 Gorkha earthquake, Nepal. Geomorphology 301:121–138

Robbins JC (2016) A probabilistic approach for assessing landslide-triggering event rainfall in Papua New Guinea, using TRMM satellite precipitation estimates. J Hydrol 541:296–309

Roose E, Arabi M, Brahamia K, Chebbani R, Mazour M, Morsli B (1993) Érosion en nappe et ruissellement en montagne méditerranéenne algérienne. Cahiers Orstom, série pédologie 28(2):289–308

Schlögel R, Marchesini I, Alvioli M, Reichenbach P, Rossi M, Malet JP (2018) Optimizing landslide susceptibility zonation: Effects of DEM spatial resolution and slope unit delineation on logistic regression models. Geomorphology 301:10–20

Shipway ICF, Hackney GA, Baynes FJ (2015) Semi-quantitative risk assessment in road design

Solaimani K, Mousavi SZ, Kavian A (2013) Landslide susceptibility mapping based on frequency ratio and logistic regression models. Arab J Geosci 6(7):2557–2569

Stark CP, Hovius N (2001) The characterization of landslide size distributions. Geophys Res Lett 28(6):1091–1094

Thiery Y, Maquaire O, Fressard M (2014) Application of expert rules in indirect approaches for landslide susceptibility assessment. Landslides 11(3):411–424

Thiery Y, Malet JP, Sterlacchini S, Puissant A, Maquaire O (2007) Landslide susceptibility assessment by bivariate methods at large scales: application to a complex mountainous environment. Geomorphology, 92(1-2), 38-59.

Thiery Y, Terrier M, Colas B, Fressard M, Maquaire O, Grandjean G, Gourdier S (2020) Improvement of landslide hazard assessments for regulatory zoning in France: STATE–OF–THE-ART perspectives and considerations. Int J Disaster Risk Reduct 47:101562

Thomas G (1985) Géodynamique d'un bassin intramontagneux: Le Bassin du Bas-Chelif occidental (Algérie) durant le mio-plio-quaternaire (Doctoral dissertation)

Van Westen CJ, Van Asch TWJ, Soeters R (2006) Landslide hazard and risk zonation—why is it still so difficult? Bull Eng Geol Environ 65(2):167–184

Van Westen CJ, Castellanos E, Kuriakose SL (2008) Spatial data for landslide susceptibility, hazard, and vulnerability assessment: an overview. Eng Geol 102(3-4):112–131

Van Westen CJ, Alkema D, Damen MCJ, Kerle N, Kingma NC (2011) Multi-hazard risk assessment. United Nations University–ITC School on Disaster Geoinformation Management.Veh G, Cotton F, Korup O (2019) Effects of finite source rupture on landslide triggering: the 2016 M w 7.1 Kumamoto earthquake. Solid Earth 10(2):463–486

Veh G, Korup O, von Specht S, Roessner S, Walz A (2019) Unchanged frequency of moraine-dammed glacial lake outburst floods in the Himalaya. *Nat. Clim. Chang.* 9, 379–383. doi: 10.1038/s41558-019-0437-5

Voumard J, Caspar O, Derron MH, Jaboyedoff M (2013) Dynamic risk simulation to assess natural hazards risk along roads. Nat Hazards Earth Syst Sci 13(11):2763–2777

Xu C, Xu X, Dai F, Xiao J, Tan X, Yuan R (2012) Landslide hazard mapping using GIS and weight of evidence model in Qingshui river watershed of 2008 Wenchuan earthquake struck region. *Journal of Earth Science*, *23*(1), 97-120.

Yalcin A, Reis S, Aydinoglu AC, Yomralioglu T (2011) A GIS-based comparative study of frequency ratio, analytical hierarchy process, bivariate statistics and logistics regression methods for landslide susceptibility mapping in Trabzon, NE Turkey. Catena 85(3):274–287

Yan Y, Cui Y, Tian X, Hu S, Guo J, Wang Z, Yin S, Liao L (2020) Seismic signal recognition and interpretation of the 2019 "7.23" Shuicheng landslide by seismogram stations. Landslides, 17(5), 1191-1206.

Yang Z, Qiao J, Uchimura T, Wang L, Lei X, Huang D (2017) Unsaturated hydro-mechanical behaviour of rainfall-induced mass remobilization in post-earthquake landslides. Eng Geol 222:102–110

Yilmaz I (2010) Comparison of landslide susceptibility mapping methodologies for Koyulhisar, Turkey: conditional probability, logistic regression, artificial neural networks, and support vector machine. Environ Earth Sci 61(4):821–836

Zaagane M, Benhamou M, Frédéric D, Refas S, Hamimed A (2015) Morphometric analysis of landslides in the Ouarsenis area (west Algeria): implications for establishing a relationship between tectonic, geomorphologic, and hydraulic indexes. Arab J Geosci 8(9): 6465–6482

Zaagane M, Refas S, Khaldi A, Frédéric D, Hamimed A, Aissa S, Moussa K, Sebbane A, Azzaz H, Mouassa S (2016) Relationship between geo-structural evolution and development of karstic systems in the culminating area of Ouarsenis (West Algeria). Arab J Geosci 9(14): 638

Zêzere JL, de Brum FA, Rodrigues ML (1999) The role of conditioning and triggering factors in the occurrence of landslides: a case study in the area north of Lisbon (Portugal). Geomorphology 30(1-2):133–146

Zygouri V, Koukouvelas IK (2019) Landslides and natural dams in the Krathis River, north Peloponnese, Greece. Bull Eng Geol Environ 78(1):207–222